Chalcogenide Letters Vol. 9, No. 1, January 2012, p. 1 - 9

# STRUCTURAL PROPERTIES OF SILVER BOROGERMANTE SUPERIONIC GLASSY SYSTEM

M. M. ELOKR[a], ASMAA. ABDELGHANY[b], F. M. HAFEZ[b], F. AHMAD[b]
[a]*Physics Department, Faculty of Science, Al- Azhar University, Cairo, Egypt.*
[b]*Physics Department, Faculty of Science, Al -Azhar University, Girls Branch, Cairo, Egypt.*

The structure of supersonic system 50AgI-20$Ag_2O$-y$GeO_2$-(30-y)$B_2O_3$ where y = 0, 5, 10, 20, 30 mol % have been prepared and investigated by X-ray diffraction, FTIR and DSC analysis. By increasing temperature and/or heat treatment peaks due to growth of AgI microdomains are observed in XRD patterns due to α-AgI nanocrystals. IR spectra show that the addition of $GeO_2$ reduces the germanium non bridging oxygen, and enhances the formation of octahedral groups. Additionally the borate non bridging oxygen increases, and the formation of tetrahedral groups decrease. The addition of $GeO_2$ to $B_2O_3$ content enhances glass forming ability and stability.

(Received October 18, 2011; Accepted January 6, 2012)

*Keywords: superionic, germante, glassy*

## 1. Introduction

The study of superionic solids is an important field of material science and technology. Most of solids states are based on motion of electron. In contrast ionic solids have received very little attention in the past, in spite of the fact that these solids are the best to be understood by solid state physicists and chemists. The main reason for this was the non availability of solids with high ionic conductivity at room temperature. Solids with high ionic conductivity are termed as "superionic solids" or solid electrolytes [(1)]. The glassy electrolytes are a class of materials in which the cationic or anionic constituents are not confined to specific lattice sites, but are essentially free to move throughout the structure. Thus, these classes have attracted much attention because of their use for applications in solid state electrochemical devices such as rechargeable battery or microbattery operation, those needed for electric automobiles and heart pacemakers, fuel cells electrochromic devices, electrochemical sensors, smart windows and displays [(1-3)].

AgI based borate and germanate glasses have attracted much attention because of their high glass transition. The introduction of germanium content in the superionic borogermante glasses improves the glass transition temperatures and glass forming character by increasing rigidity of the network of these glasses. Besides they are promising for technological applications [(4,5)].

## 2. Experimental Work

A homogenous mixture of chemicals in appropriate mol wt compositions 50AgI-20$Ag_2O$-y$GeO_2$-(30-y)$B_2O_3$ were prepared where y=0, 5, 10, 20, 30 mol %. The samples were prepared from chemical compounds, $AgNO_3$ (Aser 99.99), $B_2O_3$ (Aldrich 99.99) $GeO_2$ (Aldrich 99.99), silver nitrate was used as starting material to yield silver oxide. AgI was prepared by reacting KI and $AgNO_3$ in dionized water [(1)]. The mixture was melted in porcelain crucible at 600-750$^oC$ for 25-30 min depending on composition. The melts were shaken several times during heating to ensure a high degree of homogeneity, and then the melts were quenched between two polished copper blocks kept at room temperature to yield the homogeneous glasses.

The samples were examined to test the amorphous nature using BUKER axs X-ray analytical diffraction system, type D8 ADVANCE supplied with furnace attachment. The diffraction system based with Cu tube anode of wave length $K\alpha_1$= 1.5460 Å and $K\alpha_2$= 1.54439 Å. The start angle (2θ) was $10^o$ and the end angle was $60^o$.

Infrared measurements were done by using AT/Mottson - Genesis Series FTIR spectrometer, in the range (200-4000 $cm^{-1}$). IR spectra of powdered samples were obtained in a potassium bromide (KBr) pellets. Careful grinding of the sample is of a great importance for the elimination of errors caused by scattering. The concentration of the sample can be adjusted accurately in the pellet by amount ~1/99 from KBr; the pellet of KBr is taken as a reference to avoid the impurities of the used KBr.

The thermal measurements were carried out by using Shimadzu DSC-50 Analyzer on finely powdered glass samples. This was carried out with a heating rate 10 $^oC$/min in the temperature range from (room temperature - 500 $^oC$).

The glass forming ability (GFA) and stability (GFS) can be determined from the thermograms $T_g$ & $T_x$ & $T_p$ as [6]:

$$GFA = T_X - T_g \quad \& \quad GFS = (T_X - T_g)(T_p - T_x)/T_g \qquad (1)$$

## 3. Results and Discussion

### 3.1 X-ray diffraction

Representative X-ray diffraction (XRD) patterns obtained at room temperature are illustrated in figure (1). No sharp peaks are observed, reflecting the amorphous nature of the prepared samples. Figure (2) shows XRD patterns for the rapidly quenched of y=10% glass measured at various temperatures of 32 (a), 100 (b), 150 (c), 200 (d), and 300 $^oC$ (e) by a high temperature XRD apparatus in the heating process. No diffraction peaks are observed at 32$^oC$. On the other hand, peaks of α-AgI (body centered cubic) start to appear at 100$^oC$. The intensity of the latter increases by raising temperature. It should be mentioned that the solubility of AgI in glass is low and small crystals of AgI can be observed without any heat treatment [7]. Recent studies as Raman and NMR suggest that the existence of α-AgI nanocrystals small clusters or microdomains of an amorphouslike AgI with tetrahedral coordination similar to that of crystalline superionic α-AgI, speatially at high AgI concentration [1,8,9]. Also there are unidentified peak, denoted by □ in figure (2) (d,e), similar peaks which was observed by M. Tatsumisago and et al [7].

Figure (3) shows the room temperature XRD patterns of the as prepared and heat treated (the sample had heated at 180$^oC$ for 8 h) of y= 10% samples, the samples are treated and consecutively cooled down to room temperature. The XRD pattern shows that, for y= 10% the heat treatment leads to intense peaks due to formation of β-AgI (hexagonal structure). Such β-AgI crystals are usually formed mainly on the surface of the glass [7].

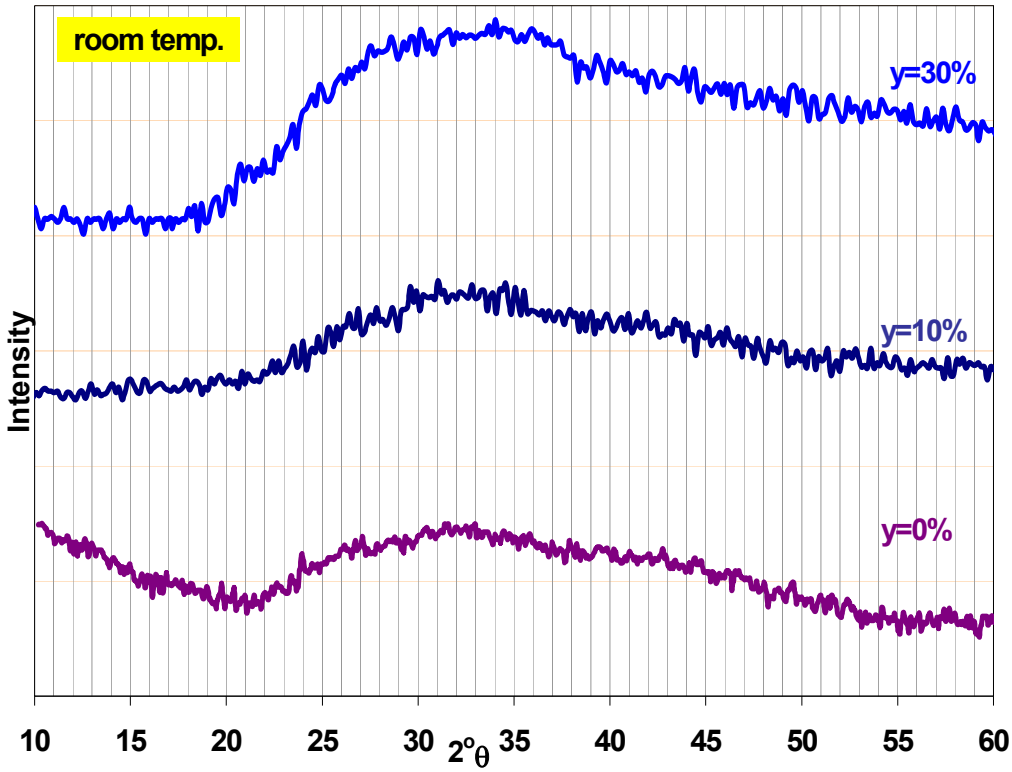


*Fig. (1) X-ray diffraction pattern for some samples at room temperature.*

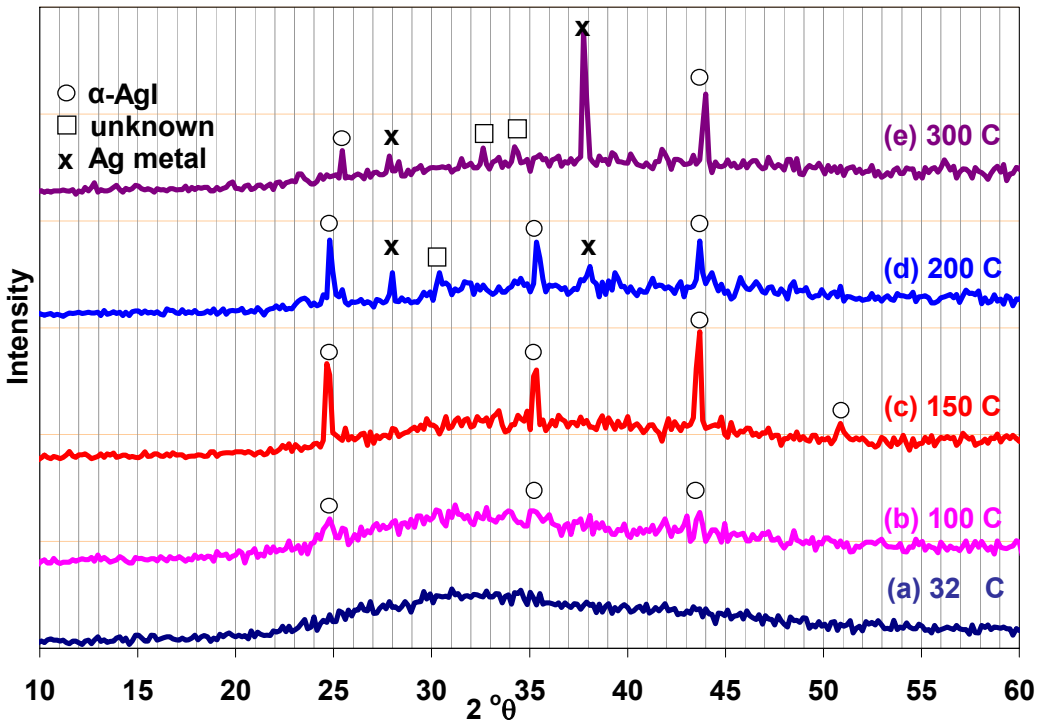


*Fig. (2) X-ray diffraction pattern for y=10% sample at different temperatures during the heating process.*

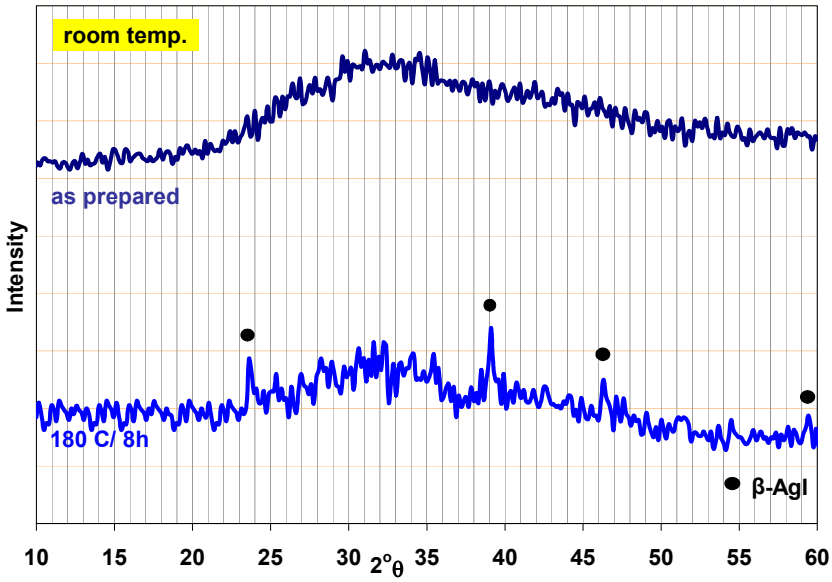


*Fig. (3) X-ray diffraction pattern for as prepared and heat treatment for y=10%.*

### 3.2. Deferential scanning calorimetric (DSC)

DSC thermograms of the investigated samples are illustrated in figure (4). The obtained thermograms follow one common pattern where endothermic peaks characteristic for glass transition ($T_g$). Exothermic peaks corresponding to the crystallization temperature ($T_x$) is also observed, the latter centered at $T_p$ corresponding to peak top.

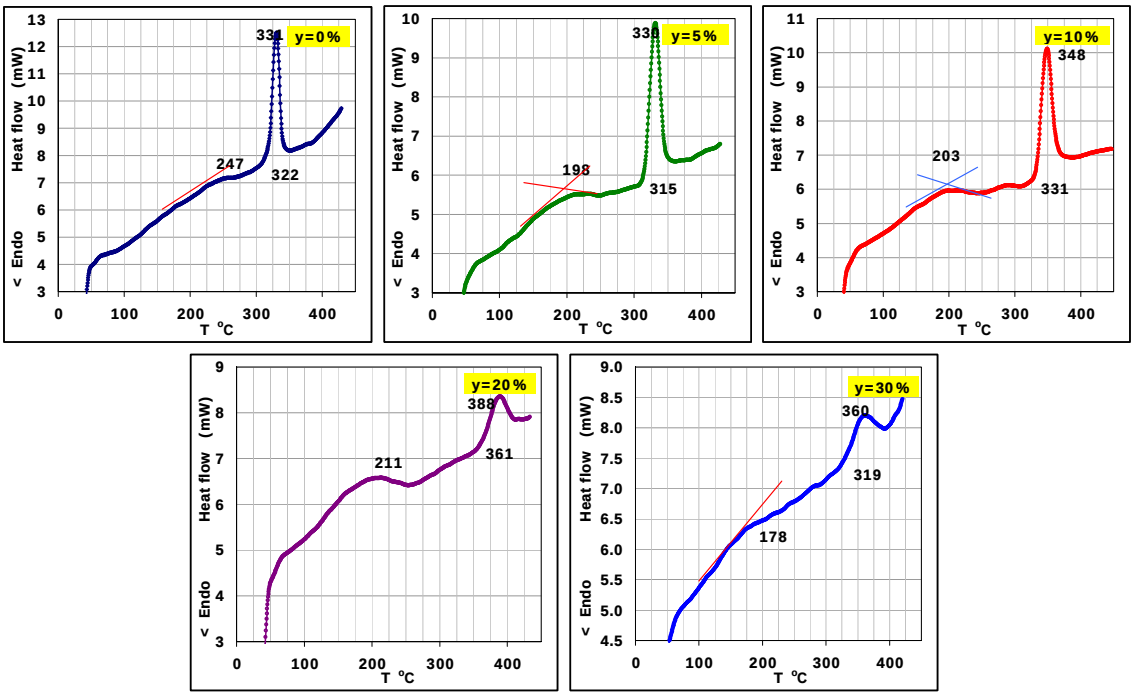


*Fig. (4) DSC thermograms for all samples with different $GeO_2$ content.*

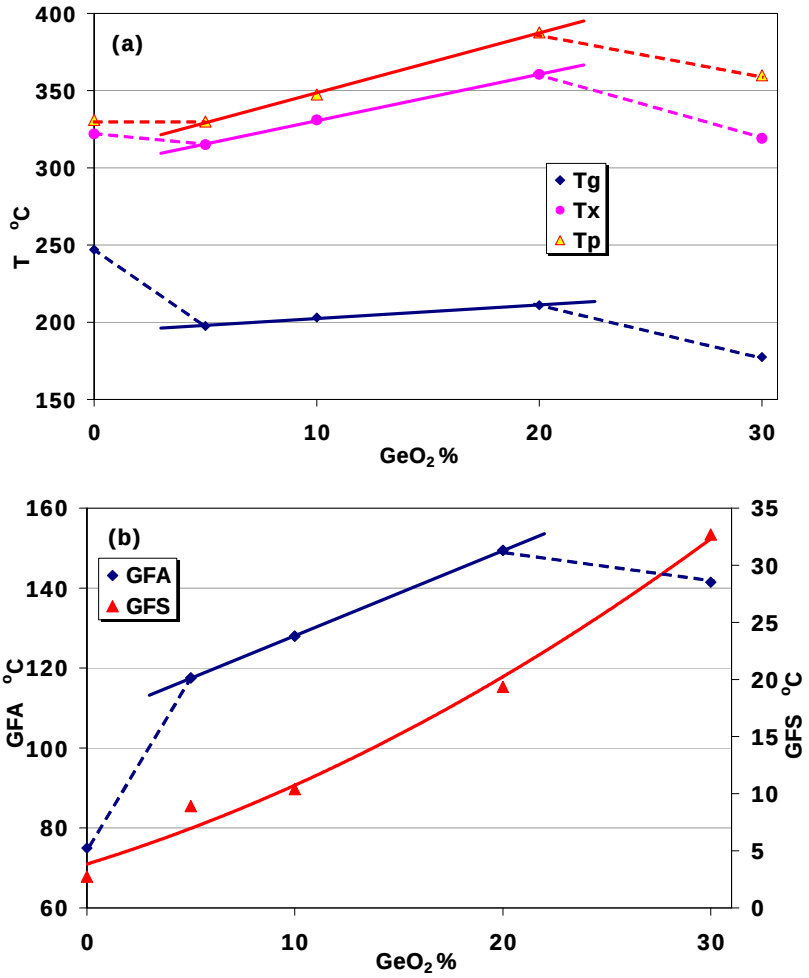


*Fig. (5) (a) DSC variables $T_g$, $T_x$, $T_p$, (b) GFA and GFS as a function of $GeO_2$ content.*

The pure borate glass sample (y=0%) shows higher $T_g$ than that of pure germinate glass sample (y=30%) [5]. This may be attributed to the ionic radii of Ge cation which is larger than that of B cation. However the borogermanate samples show $T_g$'s lower than pure borate sample. Such considerable difference in ionic radii can cause breaking of boron-oxygen bridges [10,11]. The crystallization temperature shows the same the behavior. While in the interval $0<GeO_2>30$ (mixed borogermanate), the introduction of $GeO_2$ causes increament in the $T_g$, $T_x$, $T_p$, that may be due to change of Ge coordination from four to six; to cause relative compaction in glass structure and decrease of the average size of voids. Hence, increasing of rigidity of the network of these glasses in this interval as showed in figure (5a) [12- 14].

The calculated glass forming ability and stability according to equation (1) are plotted as a function of $GeO_2$ content is shown in figure (5b). It is clear that the addition of $GeO_2$ to $B_2O_3$ content enhance both of them [5].

### 3.3. Infra-red (IR) absorption results

Figure (6) shows the IR absorption spectra over frequency range 300-1600 $cm^{-1}$. The IR spectra show overlapped broad absorption bands, which indicate an amorphous structure of the studied samples [1,10,15].

To explain the origin of this characteristic infrared symmetry, the spectra are deconvoluted using Gaussian components which give the best fit using non-linear least squares fitting method. The spectra of all samples show a strong and wide absorption band in the region 1570- 1180 $cm^{-1}$ is usually connected with the B-O-B stretching vibrations mode of polymerized $BO_3$.This band consists of two types; the first type is borate triangles non bridging oxygens (NBO's) ca. ~1240 and 1450 $cm^{-1}$, the second type is the normal borate

triangles bridging oxygens which locate at the center of triangles band. While broad band observed in the region 1180-790 $cm^{-1}$ is most probably due to B-O stretching and rocking motion vibration of tetrahedral ($BO_4$) groups. A very weak band below 800 $cm^{-1}$ was also observed and it could be attributed to bending vibration of $BO_3$ groups [1,16-18].

The inflection at about 1110 $cm^{-1}$ is related to stretching vibrations of Ge-O-B when boron and germanium are in tetrahedral coordination. The bands at around 850 and 770 $cm^{-1}$ correspond to $GeO_4$ and $GeO_6$, respectively [1,10,11,15,19,20]. The band ~640 $cm^{-1}$ may be due to the stretching vibration mode of tetrahedra non bridging oxygens ($Ge\text{-}O^-$ bond). The other bands at 350 and 490 $cm^{-1}$ are due to the bending mode of bridging oxygen atoms and deforming vibrations of O-Ge-O bond with tetrahedral units, respectively [1,10,15,21].

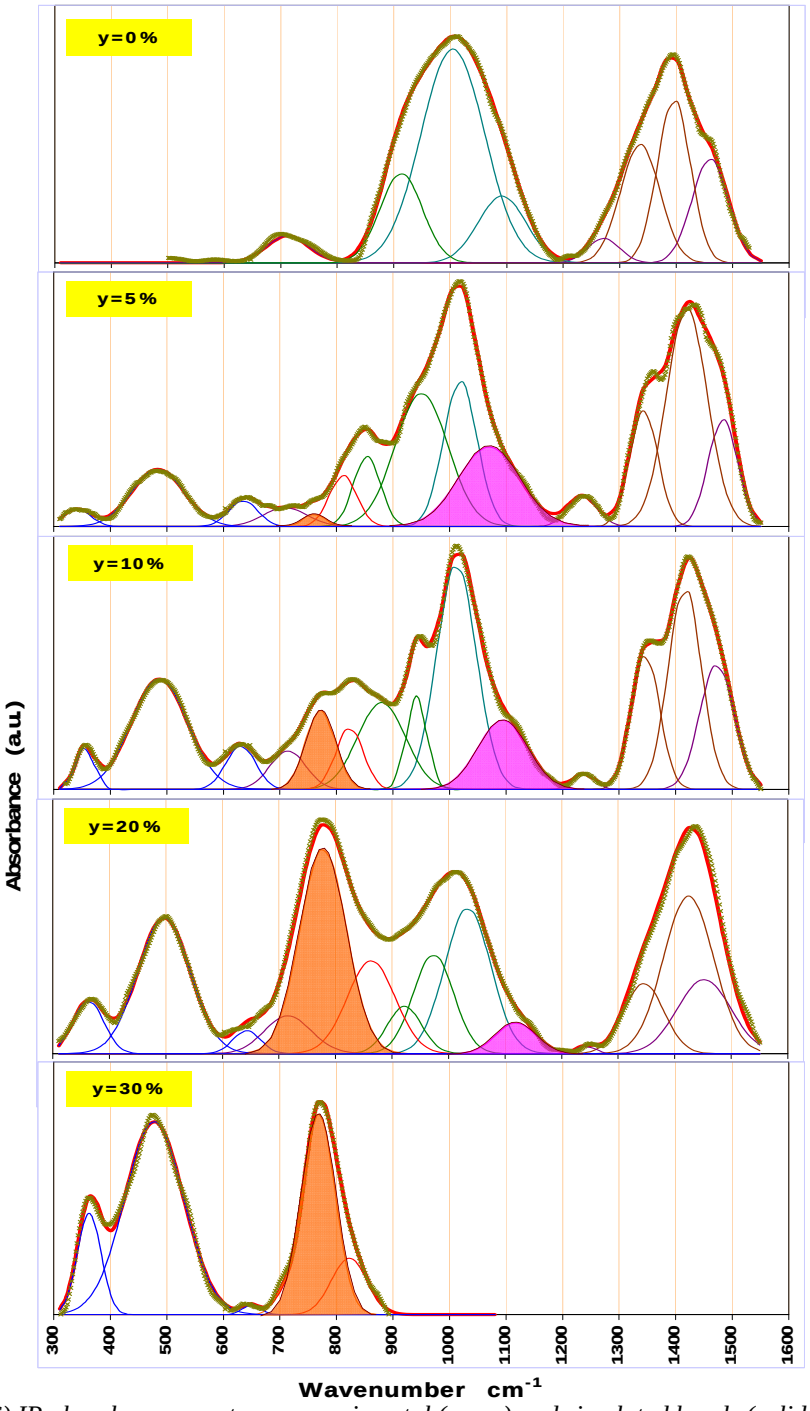


*Fig. (6) IR absorbance spectrum, experimental (cross) and simulated bands (solid lines).*

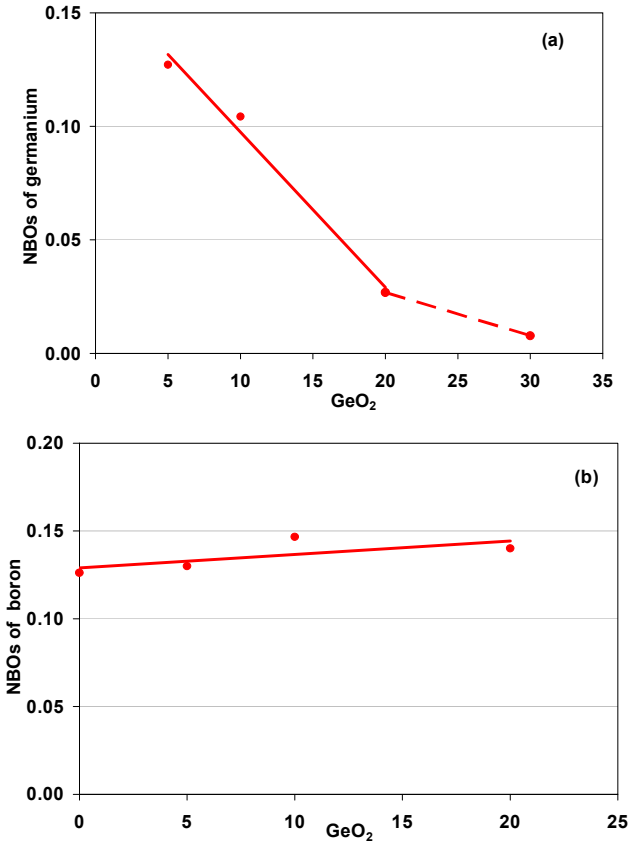


*Fig. (7) NBOs as a function $GeO_2$ content for (a) germanium, (b) boron.*

Figure (7) shows that, the additions of $GeO_2$ give more NBO's in boron triangles by converting some of $BO_4$ to $BO_3$ units, and converting the germanium NBO's to $GeO_6$ units. The formation of non-bridging B-$O^-$ bonds may be due to the increase of $GeO_6$. The ionic radii of the cations: $B^{+3}$ (in tetrahedral coordination), $Ge^{+4}$ (in tetrahedral coordination) and $Ge^{+4}$ (in octahedral coordination) are 0.25, 0.53 and 0.67 Å, respectively [22]. Such a considerable difference in ionic radii can cause, with a great number of $GeO_6$ octahedral, breaking of boron-oxygen bridges [10]. In the pure germanium sample (y=30%) the $GeO_6$ units are decreased, due to change of Ge coordination from six to four; to cause relative expansion in glass structure and increase of the average size of voids. Hence, decreasing of rigidity of this sample network result in low glass transition temperature as shown previously in the DSC.

In this respect it is observed that, the introduction of $GeO_2$ up to 20% leads to the increase of the envelope intensity of octahedral $GeO_6$ units [$N_{G6}$=concentration of $GeO_6$ /( $GeO_6$ + $GeO_4$)] relative to those tetrahedrall units [$N_{G4}$=concentration of $GeO_4/(GeO_6+GeO_4)$] and the decrease of the intensity of tetrahedral $BO_4$ units [$N_{B4}$=concentration of $BO_4/(BO_3+BO_4)$] relative to those triangles $BO_3$ [$N_{B3}$=concentration of $BO_3/(BO_3+BO_4)$] units. At y=30% the values of $N_{G6}/N_{G4}$ decrease as shown in figure (8).

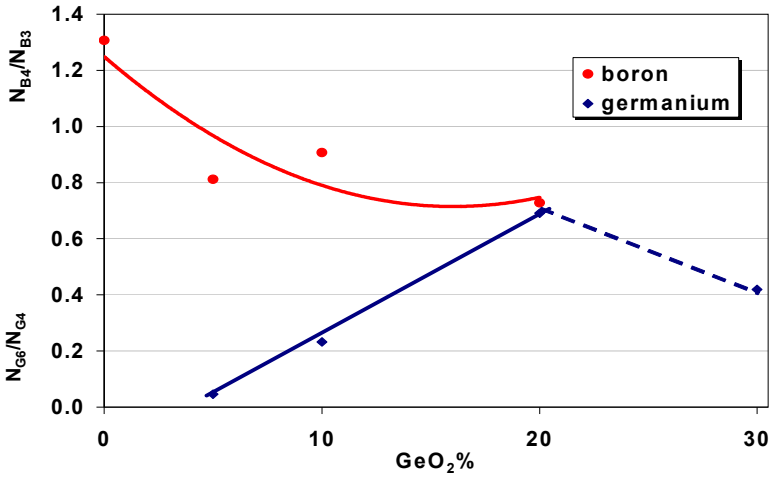


*Fig. (8) The $N_{B4}/N_{B3}$ and $N_{G6}/N_{G4}$ as a function of $GeO_2$ content.*

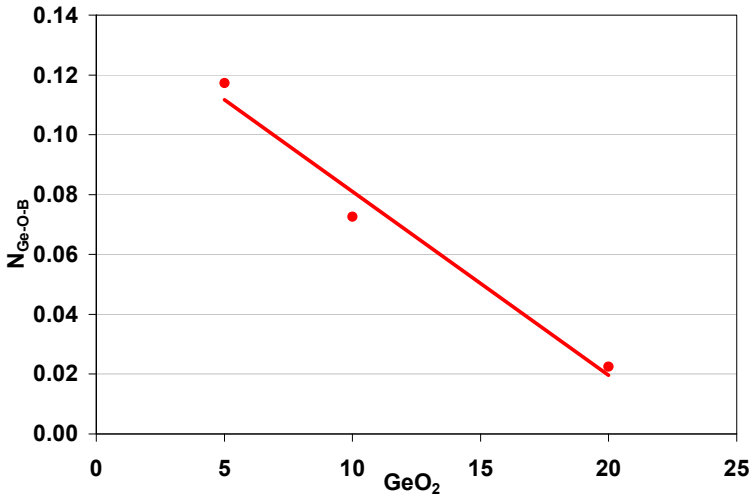


*Fig. (9) Ge-O-B band as a function of $GeO_2$ content.*

Figure (9) shows the composition dependence of the Ge-O-B band intensity, it decreases by increasing $GeO_2$ which may be due to breakdown of six membered ring of $BO_4$ group [5,10].

## 4. Conclusion

No diffraction peaks were observed in X-ray pattern of the investigated samples at room temperature indicating their amorphous nature. Peaks due to growth of AgI microdomains are observed in X-ray pattern by increasing temperature and heat treatment. The addition of $GeO_2$ to $B_2O_3$ content enhances glass forming ability and stability. The addition $GeO_2$ reduces the germanium non bridging oxygen, and enhances the formation of octahedral groups. On the other hand, the addition $GeO_2$ increases the borate non bridging oxygen, and decrease the formation of tetrahedral groups.

## References

[1] J.J. Hudgens, S.W. Martin, Physical Review B, V. **53**(9), 5348 (1996).
[2] C.S. Sunandana, S. Kumar, Bull. Mater. Sci., V. **27**(1), 1 (2004).

[3] P. Boolchand, W.J. Bresser, Nature, V. **410**(26), 1070 (2001).
[4] T. Minami, Y. Ikeda, M. Tanaka, J. of Non-Cryst. Solids, **52**, 159 (1982).
[5] Q. Mei, Jason Saienga, Jeremy Schrooten, Steve W. Martin, J. of Non-Cryst. Solids, **324**, 264 (2003).
[6] N.C. De Souza, R. Lebullenger, M.C.C. Custodio, A.C. Hernandes, J. Non- Cryst. Solids **273**, 94 (2000).
[7] M. Tatsumisago. T. Saito, T. Minami, Phys. Chem. Glasses, 42(3) (2001) 215-219.
[8] N. Kuwata, J. Kawamura, Y. Nakamura, K. Okuda, M. Tatsumisago, T. Minami, Solid State Ionics, **136-137,** 1061 (2000).
[9] L. Börjesson, Physical Review B, V. **36**(9), 4600 (1987).
[10] K. Blaszczak, A. Adamczyk, W. Jelonek J. of molecular Structure **511-512,** 163 (1999).
[11] T. Minami, K. Imazawa and M. Tanaka, J. of Non-Cryst. Solids, **42**, 469 (1980).
[12] Y.D. Yiannopoulos, C.P.E. Varsamis, E.I. Kamitsos Chemical Physical Letters **359**, 246 (2002).
[13] H. J. Weber J. of Non-Cryst. Solids, **243**, 220 (1999).
[14] Q. Mei, B. Meyer, D. Martin, S. W. Martin, Solid State Ionics, **168**, 75 (2004).
[15] K. Blaszczak, A. Adamczyk, M. Wedzikowska, M. Rokita, J. of molecular Structure **704**, 275 (2004).
[16] C.P. Varsamis, E.I. Kamitsos, G.D. Chryssikos, Solid State Ionics, **136-137**, 1031 (2000).
[17] C.P. Varsamis, E.I. Kamitsos, G.D. Chryssikos, Physical Review B, V. **60**(6), 3885 (1999).
[18] S. Bhattacharya, A. Ghosh, Chemical Physics Letters, **424**, 295 (2006).
[19] D.Di martino, L.F. Santors, A.C. Marques, R.M Almeida, J. of Non-Cryst. Solids, **293-295,** 394 (2001).
[20] S. Simon, I. Ardelean, I. Bratu, Solid state communications, **116**, 83 (2000).
[21] E. E. Khawaja, M.S. Hussain, M.N. Khan, J. of Non-Cryst. Solids, **79**, 275 (1986).
[22] S. Giri, C. Gaebler, J. Helmus, M. Affatigato, S. Feller, M. Kodama, J. of Non-Cryst. Solids, **347**, 87 (2004).